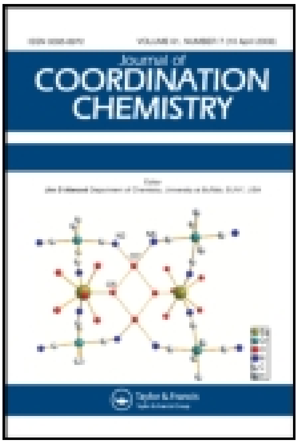

Journal of Coordination Chemistry
Publication details, including instructions for authors and subscription information:
http://www.tandfonline.com/loi/gcoo20

Syntheses, structural determination, and binding studies of mononuclear nine-coordinate $(enH_2)[Sm^{III}(egta)(H_2O)]_2 \cdot 6H_2O$ and 2-D ladder-like nine-coordinate $(enH_2)_{1.5}[Sm^{III}(ttha)] \cdot 4.5H_2O$

Jingqun Gao [a] , Dan Li [a] , Jun Wang [a] , Xudong Jin [a] , Tong Wu [a] , Kai Li [a] , Pingli Kang [a] & Xiangdong zhang [a]
[a] Department of Chemistry , Liaoning University , Shenyang 110036, P.R. China

To cite this article: Jingqun Gao , Dan Li , Jun Wang , Xudong Jin , Tong Wu , Kai Li , Pingli Kang & Xiangdong zhang (2011) Syntheses, structural determination, and binding studies of mononuclear nine-coordinate $(enH_2)[Sm^{III}(egta)(H_2O)]_2 \cdot 6H_2O$ and 2-D ladder-like nine-coordinate $(enH_2)_{1.5}[Sm^{III}(ttha)] \cdot 4.5H_2O$, Journal of Coordination Chemistry, 64:13, 2234-2245, DOI: 10.1080/00958972.2011.594888

To link to this article: http://dx.doi.org/10.1080/00958972.2011.594888

Journal of Coordination Chemistry
Vol. 64, No. 13, 10 July 2011, 2234–2245

Syntheses, structural determination, and binding studies of mononuclear nine-coordinate $(enH_2)[Sm^{III}(egta)(H_2O)]_2 \cdot 6H_2O$ and 2-D ladder-like nine-coordinate $(enH_2)_{1.5}[Sm^{III}(ttha)] \cdot 4.5H_2O$

JINGQUN GAO, DAN LI, JUN WANG*, XUDONG JIN, TONG WU, KAI LI, PINGLI KANG and XIANGDONG ZHANG

Department of Chemistry, Liaoning University, Shenyang 110036, P.R. China

(*Received 4 May 2011; in final form 6 May 2011*)

Two lanthanide complexes, $(enH_2)[Sm^{III}(egta)(H_2O)]_2 \cdot 6H_2O$ (**1**) (en = ethylenediamine and H_4egta = ethyleneglycol-bis-(2-aminoethylether)-*N*,*N*,*N*′,*N*′-tetraacetic acid) and $(enH_2)_{1.5}[Sm^{III}(ttha)] \cdot 4.5H_2O$ (**2**) (H_6ttha = triethylenetetramine-*N*,*N*,*N*′,*N*″,*N*‴,*N*‴-hexaacetic acid), have been synthesized and characterized by IR spectroscopy, thermal analysis, and single-crystal X-ray diffraction. The $(enH_2)[Sm^{III}(egta)(H_2O)]_2 \cdot 6H_2O$ is mononuclear nine-coordinate and crystallizes in the monoclinic crystal space group $P2_1/n$ with the cell dimensions $a = 13.0563(13)$ Å, $b = 12.6895(11)$ Å, $c = 14.9497(15)$ Å, $\beta = 105.782(2)°$. The polymeric $(enH_2)_{1.5}[Sm^{III}(ttha)] \cdot 4.5H_2O$ is also nine-coordinate crystallizing in the monoclinic crystal space group $P2_1/n$, but with cell dimensions $a = 17.7800(16)$ Å, $b = 9.7035(10)$ Å, $c = 22.096(2)$ Å, $\beta = 118.8740(10)°$. Each ethylenediammonium (enH_2^{2+}) cation in $(enH_2)[Sm^{III}(egta)(H_2O)]_2 \cdot 6H_2O$ connects three adjacent $[Sm^{III}(egta)(H_2O)]^-$ anions through hydrogen bonds, while in $(enH_2)_{1.5}[Sm^{III}(ttha)] \cdot 4.5H_2O$, there are two types of enH_2^{2+} cations, which form hydrogen bonds with the neighboring $[Sm^{III}(ttha)]^{3-}$ anions, leading to the formation of a 2-D ladder-like layer structure.

Keywords: Samarium ion (Sm^{III}); Ethyleneglycol-bis-(2-aminoethylether)-*N*,*N*,*N*′,*N*′-tetraacetic acid (H_4egta); Triethylenetetramine-*N*,*N*,*N*′,*N*″,*N*‴,*N*‴-hexaacetic acid (H_6ttha); Ethylenediamine (en); Hydrogen bond

1. Introduction

The syntheses of complexes containing lanthanides are of particular interest because of their flexible coordination geometry and potential applications in catalysis, gas storage, magnetism, and optics [1–5]. Tb(III), with a variety of organic ligands, are luminescent probes for fluoroimmuno-assays [6, 7]. Eu(III) complexes are promising for light-emitting layers of electroluminescent devices [8–10]. The radioactive $^{153}Sm^{III}$ ion, with favorable chemistry and physical characteristics, such as half-life of 46.27 h, β- and

---

*Corresponding author. Email: wangjuncomplex890@126.com

Journal of Coordination Chemistry
ISSN 0095-8972 print/ISSN 1029-0389 online
DOI: 10.1080/00958972.2011.594888

γ-emissions with moderate energy [11], makes it with various ligand systems an attractive candidate for tumor therapy of brain, liver, lung, and bone tissue [12, 13]. $^{153}Sm^{III}$-EDTMP (EDTMP = ethylenediamine- N,N,N',N'-tetramethylenephosphonate) has been reported to have high-efficiency and long-lasting treatment of nasopharyngeal, breast carcinoma, lung cancer, and prostate carcinoma [14, 15]. $[(Me_3Si)_2NC(NPr^i)_2]_2Sm(BH_4)_2Li(thf)_2$ has high catalytic activity for the polymerization of methyl methacrylate [16]. Yan and Xie [17] reported $Sm(Nic)_3(DMF) \cdot H_2O$ (HNic = pyridine-3-carboxylic acid, DMF = N,N-dimethylformamide), which exhibits fascinating photophysical properties, might be suitable for application as new luminescent materials. Taking into account that chemical properties and applications of lanthanide complexes strongly depend on their structures, it is of interest to study the coordination environment of Sm(III) complexes. The trivalent lanthanide ions, with high coordination number and flexible coordination geometry, form stable complexes with ligands containing both OH and COOH. Therefore, aminopolycarboxylic acids, with N and O as well as COOH groups, are good candidates for constructing lanthanide complexes [18]. Herein, two aminopolycarboxylic acids (H_4egta = ethyleneglycol-bis-(2-aminoethylether)-N,N,N',N'-tetraacetic acid) and H_6ttha (=triethylenetetramine-N,N,N',N'',N''',N'''-hexaacetic acid) have been selected to research the structures of Sm(III) complexes.

Generally, the lanthanide complexes with aminopolycarboxylic acids adopt eight-, nine-, and ten-coordinate structures. In a given oxidation state (e.g., trivalent lanthanide metal ions), the coordinate structure and coordination number of lanthanide metal complexes largely depend on ionic radii, electron configuration, nature of counter cation(s), as well as shape of ligands [19–21]. Sm(III), with relatively large ionic radius and electronic configuration of f^5, tends to form nine-coordinate structures with H_6ttha and H_4egta like those with other aminopolycarboxylic acid ligands, such as $Na[Sm^{III}(edta)(H_2O)_3] \cdot 5H_2O$ (H_4edta = ethylenediamine-N,N,N',N'-tetraacetic acid) [22], $K[Sm^{III}(edta)(H_2O)_3] \cdot 2H_2O$ [23], and $Na_2[Sm^{III}(cydta)][Sm^{III}(cydta)(H_2O)_3] \cdot 11H_2O$ (H_4cydta = *trans*-1,2-cyclohexanediamine-N,N,N',N'-tetraacetic acid) [24].

In order to extend our research, two complexes, $(enH_2)[Sm^{III}(egta)(H_2O)]_2 \cdot 6H_2O$ (**1**) and $(enH_2)_{1.5}[Sm^{III}(ttha)] \cdot 4.5H_2O$ (**2**), were synthesized. As expected, both adopt nine-coordinate pseudo-monocapped square antiprisms with monoclinic space group $P2_1/n$. Like most Sm^{III} complexes with aminopolycarboxylic acid ligands, $(enH_2)[Sm^{III}(egta)(H_2O)]_2 \cdot 6H_2O$ (**1**) is a mononuclear nine-coordinate pseudo-monocapped square antiprism, while the polymeric $(enH_2)_{1.5}[Sm^{III}(ttha)] \cdot 4.5H_2O$ (**2**) adopts a 2-D ladder-like network through hydrogen bonds formed between ethylenediamine and $[Sm^{III}(ttha)]^{3-}$. Therefore, it can be seen that the ligand structures play a crucial role on the coordinate structure of lanthanide metal complexes.

2. Experimental

2.1. *Syntheses*

2.1.1. $(enH_2)[Sm^{III}(egta)(H_2O)]_2 \cdot 6H_2O$ (1). H_4egta (=ethyleneglycol-bis-(2-aminoethylether)-N,N,N',N'-tetraacetic acid) (A.R., Beijing SHLHT Science & Trade

Co., Ltd., China) (1.9017 g, 5.0 mmol) was added to 100 mL warm water and Sm_2O_3 powder (99.999%, Yuelong Rare Earth Co., Ltd., China) (0.8718 g, 2.5 mmol) was added slowly. The solution became transparent after the mixture had been stirred and refluxed for 15.0 h, and then the pH was adjusted to 6.0 by dilute ethylenediamine (en) aqueous solution. Finally, the solution was concentrated to 25 mL. A light yellow crystal appeared after 3 weeks at room temperature.

2.1.2. $(enH_2)_{1.5}[Sm^{III}(ttha)]\cdot 4.5H_2O$ (2).

H_6ttha (=triethylenetetramine-*N*,*N*,*N*′, *N*″,*N*‴,*N*‴-hexaacetic acid) (A.R., Beijing SHLHT Science & Trade Co., Ltd., China) (2.4723 g, 5.0 mmol) was added to 100 mL warm water and Sm_2O_3 powder (99.999%, Yuelong Rare Earth Co., Ltd., China) (0.8718 g, 2.5 mmol) was added slowly. After the mixture had been stirred and refluxed for 18.0 h, the solution became transparent and then the pH was adjusted to 6.0 by dilute ethylenediamine (en) aqueous solution. Finally, the solution was concentrated to 25 mL. A light-yellow crystal appeared after 2 weeks at room temperature.

2.2. *FT-IR spectra*

H_4egta, H_6ttha, $(enH_2)[Sm^{III}(egta)(H_2O)]_2\cdot 6H_2O$, and $(enH_2)_{1.5}[Sm^{III}(ttha)]\cdot 4.5H_2O$ were skived and pressed with KBr and their infrared (IR) spectra were determined by a Shimadzu-IR 408 spectrophotometer.

2.3. *Determination of TG-DTA*

TG-DTA curves of **1** and **2** were determined by a Mettler-Toledo 851° thermogravimetric analyzer in the presence of Ar ($20\,mL\,min^{-1}$) from room temperature to 800°C at a heating rate of $20^\circ C\,min^{-1}$.

2.4. *X-ray structure determination*

X-ray intensity data were collected on a Bruker SMART CCD type X-ray diffractometer system with graphite-monochromated Mo-Kα radiation ($\lambda = 0.71073$ Å) at 298 K using φ–ω scan technique from $1.72^\circ \leq \theta \leq 26.00^\circ$. The structures were solved by direct methods. All non-hydrogen atoms were refined anisotropically by full-matrix least-squares. All calculations were performed by the SHELXTL-97 program on PDP11/44 and Pentium MMX/166 computers. The crystal data and structure refinements for the complexes are listed in table 1. Hydrogens, except those of water, were generated geometrically and located in calculated positions. The crystal shows disorder in the water molecules for **2**. Selected bond distances and angles of **1** and **2** are listed in table 2. Some important hydrogen bond distances (Å), bond angles (°) and symmetry codes are listed in table 3.

Table 1. Crystal data and structure refinement for **1** and **2**.

Complex	**1**	**2**
Empirical formula	$C_{15}H_{33}N_3O_{14}Sm$	$C_{21}H_{48}N_7O_{16.50}Sm$
Formula weight	629.79	813.01
Temperature (K)	298(2)	298(2)
Wavelength (Å)	0.71073	0.71073
Crystal system	Monoclinic	Monoclinic
Space group	$P2_1/n$	$P2_1/n$
Unit cell dimensions (Å, °)		
a	13.0563(13)	17.7800(16)
b	12.6895(11)	9.7035(10)
c	14.9497(15)	22.096(2)
β	105.782(2)	118.8740(10)
Volume (Å^3), Z	2383.5(4), 4	3338.3(6), 4
Calculated density, ρ_{Calcd} (mg m^{-3})	1.755	1.618
Absorption coefficient (mm^{-})	2.535	1.839
$F(000)$	1272	1668
Crystal size (mm^3)	0.43 × 0.28 × 0.15	0.20 × 0.10 × 0.06
θ range for data collection (°)	1.84–25.02	2.35–25.02
Limiting indices	$-15 \le h \le 12$;	$-21 \le h \le 16$;
	$-15 \le k \le 14$;	$-11 \le k \le 10$;
	$-17 \le l \le 15$	$-21 \le l \le 26$
Reflections collected	11,758	17,188
Independent reflections	4211 [R(int) = 0.0284]	5898 [R(int) = 0.0610]
Completeness to θ_{max} (%)	100.0	99.9
Max. and min. transmission	0.7023 and 0.4086	0.8977 and 0.7100
Goodness-of-fit on F^2	1.084	1.084
Final R indices [$I > 2\sigma(I)$]	$R_1 = 0.0255$,	$R_1 = 0.0689$,
	$wR_2 = 0.0503$	$wR_2 = 0.1957$
R indices (all data)	$R_1 = 0.0401$,	$R_1 = 0.0971$,
	$wR_2 = 0.0583$	$wR_2 = 0.2190$
Largest difference peak and hole (e Å^{-3})	0.857 and −0.479	1.601 and −1.463
Absorption correction	Empirical	
Refinement method	Full-matrix least-squares on F^2	

3. Results and discussion

3.1. *FT-IR spectra*

3.1.1. $(enH_2)[Sm^{III}(egta)(H_2O)]_2 \cdot 6H_2O$ (1). A comparison of FT-IR spectra between H_4egta and **1** (figure S1(I)) shows ν(C–N) at 1092 cm^{-1}, red-shifted (41 cm^{-1}) compared with that (1133 cm^{-1}) of H_4egta, indicating coordination of nitrogen of H_4egta to Sm^{III}. The spectrum of free H_4egta shows a strong band at 1738 cm^{-1} from ν(C=O), which disappears completely in the spectrum of **1**. Also, the FT-IR spectrum of **1** displays the characteristic absorption of carboxylate at 1593 cm^{-1} for asymmetric stretching and at 1411 cm^{-1} for symmetric stretching, with the separation of 182 cm^{-1} for ν_{as}(OCO) and ν_s(OCO); these results clearly show that oxygen in carboxylates participate in coordination to Sm^{III}. Meanwhile, a strong and broad ν(OH) near 3469 cm^{-1} in **1** could be reasonably attributed to O–H stretch of hydrogen bonds.

3.1.2. $(enH_2)_{1.5}[Sm^{III}(ttha)] \cdot 4.5H_2O$ (2). A comparison of FT-IR spectra between H_6ttha and **2** (figure S1(II)) shows ν(C–N) at 932 cm^{-1}, blue-shifted (33 cm^{-1})

Table 2. Bond distances (Å) and angles (°) of **1** and **2**.

1					
Bond	d (Å)	Bond	d (Å)	Bond	d (Å)
Sm(1)–O(1)	2.405(3)	Sm(1)–O(7)	2.396(3)	Sm(1)–O(11)	2.506(3)
Sm(1)–O(3)	2.401(3)	Sm(1)–O(9)	2.555(3)	Sm(1)–N(1)	2.659(3)
Sm(1)–O(5)	2.382(3)	Sm(1)–O(10)	2.512(2)	Sm(1)–N(2)	2.675(3)
Angle	ω (°)	Angle	ω (°)	Angle	ω (°)
O(1)–Sm(1)–O(3)	90.48(9)	O(3)–Sm(1)–O(11)	69.32(9)	O(7)–Sm(1)–N(1)	76.78(9)
O(1)–Sm(1)–O(5)	79.95(9)	O(3)–Sm(1)–N(1)	64.13(9)	O(7)–Sm(1)–N(2)	64.19(9)
O(1)–Sm(1)–O(7)	75.30(9)	O(3)–Sm(1)–N(2)	146.90(10)	O(9)–Sm(1)–O(10)	66.99(8)
O(1)–Sm(1)–O(9)	123.96(9)	O(5)–Sm(1)–O(7)	127.92(9)	O(9)–Sm(1)–O(11)	81.03(9)
O(1)–Sm(1)–O(10)	137.33(9)	O(5)–Sm(1)–O(9)	155.72(10)	O(9)–Sm(1)–N(1)	67.48(9)
O(1)–Sm(1)–O(11)	149.16(9)	O(5)–Sm(1)–O(10)	99.13(9)	O(9)–Sm(1)–N(2)	121.57(9)
O(1)–Sm(1)–N(1)	63.45(9)	O(5)–Sm(1)–O(11)	74.96(9)	O(10)–Sm(1)–O(11)	65.46(9)
O(1)–Sm(1)–N(2)	74.13(9)	O(5)–Sm(1)–N(1)	129.31(9)	O(10)–Sm(1)–N(1)	131.56(9)
O(3)–Sm(1)–O(5)	83.55(9)	O(5)–Sm(1)–N(2)	65.24(9)	O(10)–Sm(1)–N(2)	67.25(9)
O(3)–Sm(1)–O(7)	140.65(9)	O(7)–Sm(1)–O(9)	68.61(9)	O(11)–Sm(1)–N(1)	121.75(9)
O(3)–Sm(1)–O(9)	91.40(9)	O(7)–Sm(1)–O(10)	72.12(9)	O(11)–Sm(1)–N(2)	110.09(9)
O(3)–Sm(1)–O(10)	132.07(9)	O(7)–Sm(1)–O(11)	134.87(9)	N(1)–Sm(1)–N(2)	128.08(9)
2					
Bond	d (Å)	Bond	d (Å)	Bond	d (Å)
Sm(1)–O(1)	2.412(9)	Sm(1)–O(7)	2.376(7)	Sm(1)–N(2)	2.661(10)
Sm(1)–O(3)	2.393(7)	Sm(1)–O(9)	2.409(7)	Sm(1)–N(3)	2.727(8)
Sm(1)–O(5)	2.388(7)	Sm(1)–N(1)	2.638(9)	Sm(1)–N(4)	2.667(7)
Angle	ω (°)	Angle	ω (°)	Angle	ω (°)
O(1)–Sm(1)–O(3)	84.9(3)	O(3)–Sm(1)–N(2)	73.3(3)	O(7)–Sm(1)–N(3)	63.2(2)
O(1)–Sm(1)–O(5)	149.9(3)	O(3)–Sm(1)–N(3)	137.0(3)	O(7)–Sm(1)–N(4)	76.2(2)
O(1)–Sm(1)–O(7)	71.9(3)	O(3)–Sm(1)–N(4)	137.1(2)	O(9)–Sm(1)–N(1)	124.0(3)
O(1)–Sm(1)–O(9)	75.5(3)	O(5)–Sm(1)–O(7)	135.8(2)	O(9)–Sm(1)–N(2)	135.5(3)
O(1)–Sm(1)–N(1)	63.1(4)	O(5)–Sm(1)–O(9)	77.1(2)	O(9)–Sm(1)–N(3)	124.5(2)
O(1)–Sm(1)–N(2)	130.5(3)	O(5)–Sm(1)–N(1)	126.0(3)	O(9)–Sm(1)–N(4)	64.0(2)
O(1)–Sm(1)–N(3)	134.4(3)	O(5)–Sm(1)–N(2)	65.7(3)	N(1)–Sm(1)–N(2)	67.5(4)
O(1)–Sm(1)–N(4)	95.3(3)	O(5)–Sm(1)–N(3)	72.8(2)	N(1)–Sm(1)–N(3)	111.4(3)
O(3)–Sm(1)–O(5)	76.0(3)	O(5)–Sm(1)–N(4)	83.7(2)	N(1)–Sm(1)–N(4)	149.5(3)
O(3)–Sm(1)–O(7)	142.0(2)	O(7)–Sm(1)–O(9)	124.9(3)	N(2)–Sm(1)–N(3)	67.2(3)
O(3)–Sm(1)–O(9)	74.8(3)	O(7)–Sm(1)–N(1)	76.6(3)	N(2)–Sm(1)–N(4)	130.6(3)
O(3)–Sm(1)–N(1)	66.1(3)	O(7)–Sm(1)–N(2)	99.2(3)	N(3)–Sm(1)–N(4)	67.2(2)

compared with that (899 cm^{-1}) of H_6ttha, indicating coordination of nitrogen of H_6ttha to Sm^{III}. Free H_6ttha shows a strong band at 1738 cm^{-1} from ν(C=O), which disappears completely in the spectrum of **2**. The FT-IR spectrum of **2** displays the asymmetric stretch of carboxylate at 1572 cm^{-1} and symmetric stretch at 1408 cm^{-1}, with the separation of 164 cm^{-1} for ν_{as}(OCO) and ν_s(OCO). These results clearly show that oxygen in carboxylates participate in coordination to Sm^{III}. In addition, a strong and broad ν(OH) near 3422 cm^{-1} in **2** could be reasonably assigned to O–H stretch of hydrogen bonds.

3.2. *Thermal analysis*

3.2.1. (enH$_2$)[Sm^{III}(egta)(H$_2$O)]$_2$·6H$_2$O (1). As shown in figure S2(I), the TG curve of **1** shows a three-stage decomposition pattern. The first stage weight loss is 8.08% from

Table 3. Hydrogen bond distances (Å), bond angles (°), and symmetry codes of **1** and **2**.

D–H	*d*(D–H)	*d*(H···A)	∠D–H···A	*d*(D···A)	A	Symmetry code
1						
N(3)–H(3A)	0.890	1.874	175.83	2.762	O(2)	$x+1, y, z$
N(3)–H(3B)	0.890	2.591	112.71	3.047	O(3)	$x+1/2, -y+1/2, z-1/2$
N(3)–H(3B)	0.890	1.920	168.67	2.798	O(4)	$x+1/2, -y+1/2, z-1/2$
N(3)–H(3C)	0.890	1.913	163.27	2.778	O(6)	$-x+3/2, y+1/2, -z+3/2$
2						
N(5)–H(5A)	0.890	2.174	137.93	2.896	O(13)	$-x+1, -y+1, -z+1$
N(5)–H(5B)	0.890	1.925	175.57	2.814	O(15)	–
N(5)–H(5C)	0.890	2.123	148.62	2.920	O(9)	$x, -y+1, z-1/2$
N(5)–H(5C)	0.890	2.508	114.51	2.989	O(14)	$x, -y+1, z-1/2$
N(6)–H(6A)	0.890	1.885	164.41	2.752	O(11)	–
N(6)–H(6B)	0.890	1.840	170.00	2.721	O(6)	$-x+1, -y+1, -z+1$
N(6)–H(6C)	0.890	1.907	171.53	2.791	O(4)	$x, -y+1, z-1/2$
N(7)–H(7Aa)	0.890	2.222	134.61	2.917	O(2)	$-x, y, -z+1/2$
N(7)–H(7Ba)	0.890	2.072	122.74	2.661	O(8)	–
N(7)–H(7Ca)	0.890	2.186	133.67	2.873	O(8)	$-x, y, -z+1/2$
N(7)–H(7Ca)	0.890	2.331	164.89	3.198	O(7)	$-x, y, -z+1/2$
N(8)–H(8Aa)	0.890	2.294	139.26	3.025	O(12)	–
N(8)–H(8Ba)	0.890	–	–	–	–	–
N(8)–H(8Ca)	0.890	1.898	116.36	2.428	O(16)	$-x, y, -z+1/2$
N(8)–H8(Ca)	0.890	2.594	126.08	3.200	N(8_a)	$-x, y, -z+1/2$

room temperature to 138°C, corresponding to release of six water molecules, with an endothermic peak at 104°C in the DTA curve; weight loss of 2.83% from 138°C to 184°C corresponds to the releases of two coordinated water molecules, with an endothermic peak at 148°C in the DTA curve. The second weight loss of 10.42% from 184°C to 341°C corresponds to the expulsion of ethylenediamine, with an exothermic peak at 248°C. Then, the sample gradually decomposes to 800°C (weight loss of 39.08%); the remainder is a Sm_2O_3–$Sm_2(CO_3)_3$ mixture. The overall weight loss is 60.41%.

3.2.2. $(enH_2)_{1.5}[Sm^{III}(ttha)]\cdot 4.5H_2O$ (2). As shown in figure S2(II), **2** displays similar thermal behavior, the first stage weight loss is 9.45% from room temperature to 150°C, which corresponds to the expulsion of crystal water molecules. There is a marked endothermic peak in the DTA curve at 114°C. The second weight loss of 23.84% from 150°C to 365°C corresponds to expulsion of ethylenediamine, producing two DTA peaks located at 250°C and 360°C. The last weight loss of 33.65% occurs from 365°C to 800°C, attributed to decomposition and combustion of carboxylate, with exothermic peaks at 530°C, 620°C, and 720°C; the remainder is a Sm_2O_3–$Sm_2(CO_3)_3$ mixture. The total weight loss is 66.94%.

3.3. *Molecular and crystal structures*

3.3.1. $(enH_2)[Sm^{III}(egta)(H_2O)]_2\cdot 6H_2O$ (1). Figure 1 shows the nine-coordinate structure of $(enH_2)[Sm^{III}(egta)(H_2O)]_2\cdot 6H_2O$ with a 1 : 1 metal to ligand stoichiometry, similar to that of $(enH_2)[Gd^{III}(egta)(H_2O)]_2\cdot 6H_2O$ that we had reported previously [25]. The central Sm^{III} is coordinated to two amine nitrogens and seven oxygens,

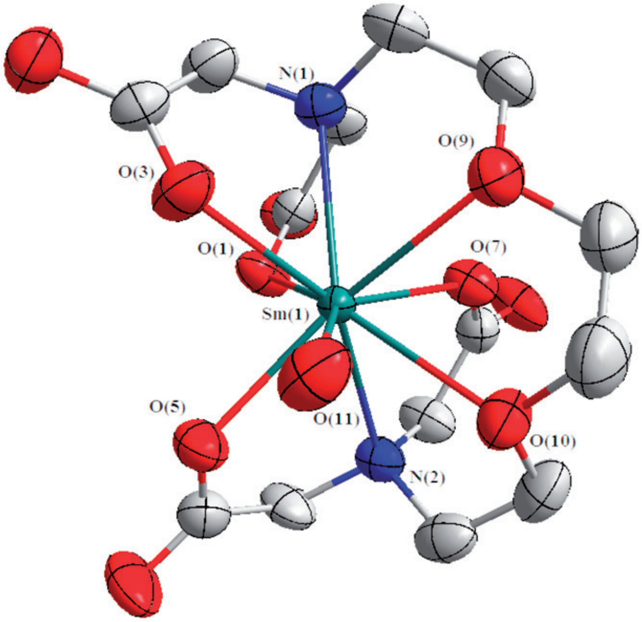

Figure 1. Molecular structure of $(enH_2)[Sm^{III}(egta)(H_2O)]_2 \cdot 6H_2O$.

of which one (O(11)) belongs to coordinated water. The remaining two amine nitrogens, four carboxyl oxygens, and two ethyleneglycol oxygens all come from one octadentate egta.

As shown in figure 2, the coordinate geometry around Sm^{III} ion, $\{SmN_2O_7\}$, can be considered as a nine-coordinate pseudo-monocapped square antiprismatic conformation with seven chelating five-membered rings. The upper square plane is formed by one ethyleneglycol O(9) and three carboxyl oxygens (O(1), O(3), and O(7)); the other plane is formed by one amine (N(2)), one carboxyl (O(5)), one ethyleneglycol (O(10)), and one coordinated water (O(11)). The capping donor is occupied by one nitrogen (N(1)). The torsion angle between the two quadrilateral planes is 39.69°.

As shown in table 2, the Sm(1)–O bond distances are considerably different, falling into the range of 2.382(3) Å (Sm(1)–O(5)) to 2.555(19) Å (Sm(1)–O(9)), and the average value is about 2.451(3) Å. Bond distances of Sm(1)–O(9) and Sm(1)–O(10) (both belonging to ethyleneglycol oxygens) are somewhat longer than other Sm(1)–O bond lengths, consistent with previously reported H_4egta [25, 26]. Also, the Sm(1)–O(11) (belonging to water) bond length of 2.506(3) Å is somewhat longer than the Sm(1)–O (belonging to carboxyl oxygens) bond lengths. The two Sm(1)–N bond distances are 2.659(3) Å (Sm(1)–N(1)) and 2.675(3) Å (Sm(1)–N(2)), with an average of 2.667(3) Å. Sm(1)–O bond distances are significantly shorter than Sm(1)–N bond distances, indicating that Sm(1)–O bonds are stronger than Sm(1)–N bonds. The O–Sm–O bond angles range from 65.46(9)° (O(10)–Sm(1)–O(11)) to 155.72(10)° (O(5)–Sm(1)–O(9)), while the O–Sm–N bond angles vary from 63.45(9)° (O(1)–Sm(1)–N(1)) to 146.90(10)° (O(3)–Sm(1)–N(2)), and the N(1)–Sm–N(2) bond angle is 128.08(9)°.

The value of dihedral angle for the top plane is 14.52° between Δ(O(1)O(3)O(7)) and Δ(O(3)O(7)O(9)), and 14.60° between Δ(O(1)O(3)O(9)) and Δ(O(1)O(7)O(9)). For the

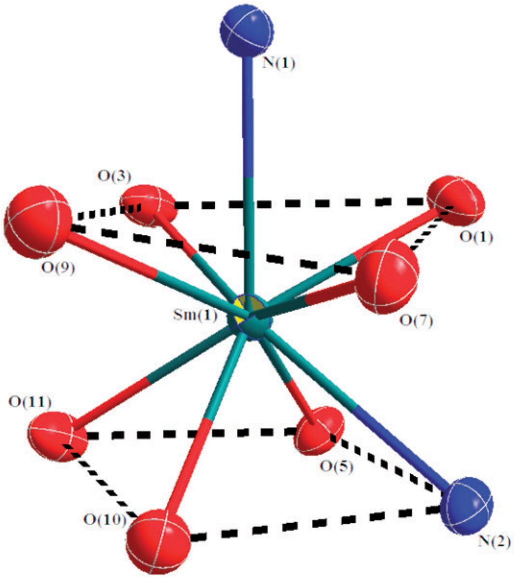

Figure 2. Coordination polyhedron around Sm(1) in **1**.

bottom plane, the corresponding value is 6.40° between Δ(O(5)O(11)N(2)) and Δ(O(10)O(11)N(2)), and 5.61° between Δ(O(5)O(10)N(2)) and Δ(O(5)O(10)O(11)). All these data confirm that the structure of $\{SmN_2O_7\}$ in **1** is a pseudo-monocapped square antiprism but distorted to a small extent according to Guggenberger and Muetterties' method [27].

As shown in figure S3, there are four $(enH_2)[Sm^{III}(egta)(H_2O)]_2 \cdot 6H_2O$ molecules in a unit cell. The complex molecules connect with one another through hydrogen bonds and electrostatic forces with crystal water and protonated ethylenediamine cations (enH_2^{2+}), and crystallize in a monoclinic system with $P2_1/n$ space group. As seen from figure S4, the enH_2^{2+} forms hydrogen bonds with four adjacent $[Sm^{III}(egta)(H_2O)]^-$ anions. Every N(3) connects four carboxyl oxygens, in which O(3) and O(4) come from the same carboxyl of one $[Sm^{III}(egta)(H_2O)]^-$, O(2) and O(6) from the other two neighboring $[Sm^{III}(egta)(H_2O)]^-$ anions, with distances of N(3)···O(2), N(3)···O(3), N(3)···O(4), and N(3)···O(6) being 2.762, 3.047, 2.798, and 2.778 Å, respectively. Owing to this special coordination environment, the Newman pattern dihedral angle of ethylenediamine is exactly 180°. Thus, four atoms of ethylenediamine all situate in the same plane.

3.3.2. $(enH_2)_{1.5}[Sm^{III}(ttha)] \cdot 4.5H_2O$ (2).

$(enH_2)_{1.5}[Sm^{III}(ttha)] \cdot 4.5H_2O$ and $(enH_2)[Sm^{III}(egta)(H_2O)]_2 \cdot 6H_2O$ have similar building units. As seen from figure 3, Sm^{III} is surrounded by four nitrogens and five oxygens, all from one ttha. There is a free (non-coordinated) carboxylate, i.e., C(17)–O(11)–O(12) in **2**, consistent with findings previously reported, such as for $Na[Tb^{III}(Httha)] \cdot 6H_2O$ [28] and $K_3[Dy^{III}(ttha)] \cdot 5H_2O$ [29].

The central Sm^{III} is nine-coordinate (figure 4) in a distorted pseudo-monocapped square antiprism with eight five-membered chelating rings. The upper square plane is

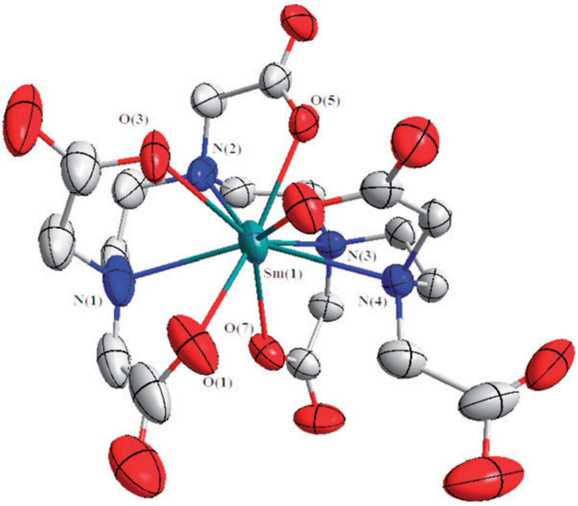

Figure 3. Molecular structure of $(enH_2)_{1.5}[Sm^{III}(ttha)] \cdot 4.5H_2O$.

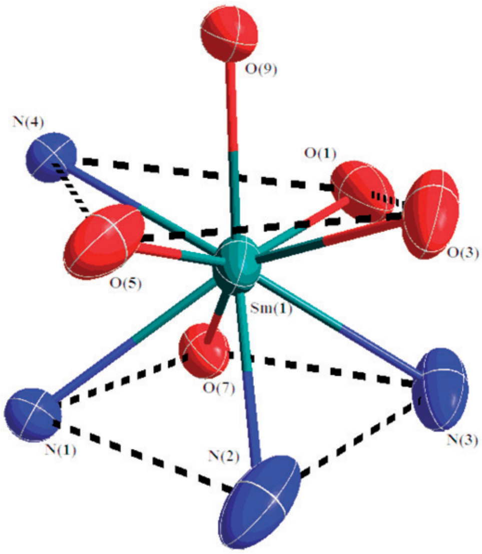

Figure 4. Coordination polyhedron around Sm(1) in **2**.

occupied by three carboxyl oxygens (O(1), O(3), O(5)) and one amine nitrogen (N(4)); the other square plane is occupied by one carboxyl (O(7)) and three amine nitrogens (N(1), N(2) and N(3)), with the capping position occupied by one carboxyl (O(9)). The torsion angle between the two quadrilateral planes is 39.13°.

As shown in table 2, the Sm(1)–O bond distances of $(enH_2)_{1.5}[Sm^{III}(ttha)] \cdot 4.5H_2O$ fall into the range 2.376(7) Å (Sm(1)–O(7)) to 2.412(9) Å (Sm(1)–O(1)), with average of 2.396(7) Å. The longest distance between Sm(1) and O(1) arises from the hydrogen bond

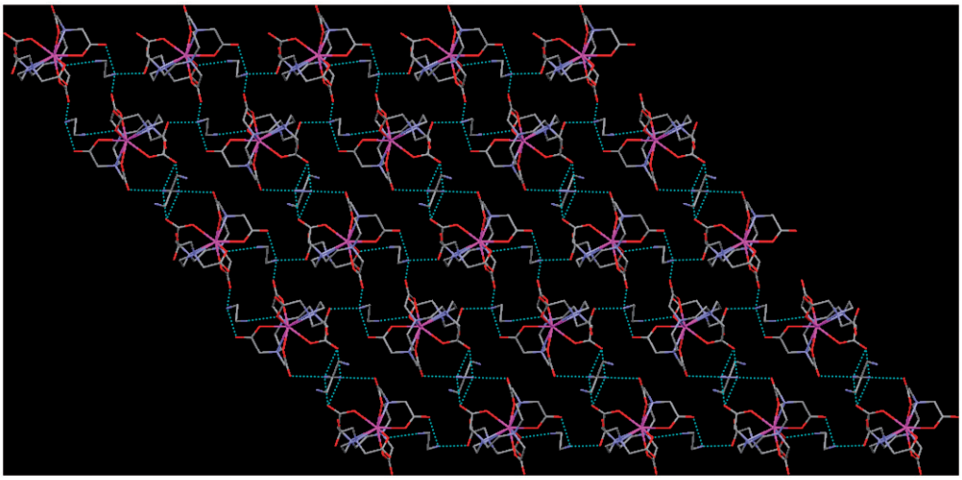

Figure 5. Polyhedral view of the 2-D ladder-like layered network of **2**.

formed between carboxyl O(1) and lattice water O(14), while the Sm(1)–N bond distances, remarkably longer than Sm(1)–O bond distances, vary from 2.638(9) Å (Sm(1)–N(1)) to 2.727(8) Å (Sm(1)–N(3)), with an average value of 2.673(9) Å. The O–Sm–O bond angles range from 71.9(3)° (O(1)–Sm(1)–O(7)) to 149.9(3)° (O(1)–Sm(1)–O(5)), the O–Sm–N bond angles vary from 63.1(4)° (O(1)–Sm(1)–N(1)) to 137.1(2)° (O(3)–Sm(1)–N(4)), and N–Sm–N bond angles range from 67.2(2)° (N(3)–Sm(1)–N(4)) to 149.5(3)° (N(1)–Sm(1)–N(4)). Among them, the largest and smallest bond angles are O(1)–Sm(1)–N(1) and O(1)–Sm(1)–O(5), respectively, because O(1) forms a hydrogen bond with the adjacent crystal water O(14), distorting $(enH_2)_{1.5}[Sm^{III}(ttha)] \cdot 4.5H_2O$.

The dihedral angle for the top plane is 14.68° between Δ(O(1)O(3)O(5)) and Δ(O(1)O(5)N(4)), and 14.78° between Δ(O(1)O(3)N(4)) and Δ(O(3)O(5)N(4)). For the bottom plane, the corresponding value is 6.56° between Δ(N(1)N(2)N(3)) and Δ(O(7)N(1)N(3)), and 5.70° between Δ(O(7)N(1)N(2)) and Δ(O(7)N(2)N(3)). According to the Guggenberger and Muetterties [27] method, it can be firmly concluded that the coordination structure of $\{SmN_2O_7\}$ in $[Sm^{III}(ttha)]^{3-}$ is a slightly distorted pseudo-monocapped square antiprism.

There are four $(enH_2)_{1.5}[Sm^{III}(ttha)] \cdot 4.5H_2O$ molecules in a unit cell (figure S5). The molecules connect through hydrogen bonds and electrostatic forces with crystal water and protonated ethylenediammonium (enH_2^{2+}), and crystallize in a monoclinic system with $P2_1/n$ space group. As seen from figure S6, there are two types of enH_2^{2+}. One enH_2^{2+} forms hydrogen bonds with three adjacent $[Sm^{III}(ttha)]^{3-}$ anions, i.e., N(5) connects with a coordinated carboxyl (O(5)) from one $[Sm^{III}(ttha)]^{3-}$, while N(6) links three carboxyl oxygens, two non-coordinated (O(4) and O(6)) and a free carboxyl (O(11)) from three different $[Sm^{III}(ttha)]^{3-}$ anions. The second enH_2^{2+}, which is highly symmetric, forms hydrogen bonds with two adjacent $[Sm^{III}(ttha)]^{3-}$ anions, with N(7) connecting two non-coordinated carboxyls (O(2) and O(8)) from one $[Sm^{III}(ttha)]^{3-}$, and one non-coordinated carboxyl (O(8)) from the other $[Sm^{III}(ttha)]^{3-}$.

As shown in figure 5, every two $[Sm^{III}(ttha)]^{3-}$ anions interconnect by sharing the highly symmetric ethylenediamine (N(7)–C(21)–C(22)–N(8)) forming a secondary building unit (SBU), with bond distances of N(7) ··· O(2), N(7) ··· O(8) (both from one neighboring $[Sm^{III}(ttha)]^{3-}$) and N(7) ··· O(8) (from the other neighboring $[Sm^{III}(ttha)]^{3-}$) being 2.917, 2.873, and 2.661 Å, respectively, and the dihedral angle of ethylenediamine is 164.47°. Two neighboring SBUs are further connected by sharing two ethylenediamines (N(5)–C(19)–C(20)–N(6)) along the *a*-axis, resulting in the formation of an infinite 1-D chain, with N(6) ··· O(4) and N(6) ··· O(6) bond distances of 2.791 and 2.721 Å, respectively. The 1-D chains are linked by sharing the ethylenediamine (N(5)–C(19)–C(20)–N(6)) in the *ac* plane, leading to the formation of a 2-D ladder-like network, with N(5) ··· O(9) and N(6) ··· O(11) bond distances of 2.920 and 2.752 Å, respectively, and the dihedral angle of 173.88°. The 2-D ladder-like network is further consolidated *via* weak hydrogen bonds between water and carboxyl oxygen as well as nitrogen from ethylenediamine to extend into a 3-D cage-like structure.

4. Conclusions

Two Sm^{III} complexes with aminopolycarboxylic acids (H_4egta = ethyleneglycol-bis-(2-aminoethylether)-*N*,*N*,*N*′,*N*′-tetraacetic acid and H_6ttha = triethylenetetramine-*N*,*N*,*N*′,*N*″,*N*‴,*N*‴-hexaacetic acid), $(enH_2)[Sm^{III}(egta)(H_2O)]_2 \cdot 6H_2O$ (**1**) and $(enH_2)_{1.5}[Sm^{III}(ttha)] \cdot 4.5H_2O$ (**2**) were synthesized and characterized by means of IR spectra, thermal analyses, and single-crystal X-ray diffraction. Compound **1** is a mononuclear nine-coordinate square antiprism and **2** is a 2-D ladder-like network with a nine-coordinate pseudo monocapped square antiprism. The change of ligands can lead to change of the structure of the complexes, coordination numbers, and coordination geometries.

Supplementary material

CCDC 800858 $(enH_2)[Sm^{III}(egta)(H_2O)]_2 \cdot 6H_2O$ and CCDC 800861 $(enH_2)_{1.5}[Sm^{III}(ttha)] \cdot 4.5H_2O$ contain the supplementary crystallographic data for this article. These data can be obtained free of charge *via* www.ccdc.cam.ac.uk/data_request/cif, by e-mailing data_request@ccdc.cam.ac.uk, or by contacting The Cambridge Crystallographic Data Centre, 12 Union Road, Cambridge CB2 1EZ, UK; Fax: +44(0)1223-336033. In addition, the IR spectroscopy, thermal analysis, arrangement of complexes in unit cell, and bindings in complexes are also provided as supplementary material.

Acknowledgments

The authors greatly acknowledge the National Natural Science Foundation of China, Liaoning Province Natural Science Foundation of Education Department, Liaoning Province Natural Science Foundation of Science and Technology Department and

Liaoning University "211" project for financial support. The authors thank their colleagues and other students for their participation in this work. Especially, they thank Professors K. Miyoshi and T. Mizuta (Faculty of Science, Hiroshima University, Japan) for instructions.

References

[1] C. Janiak. *Dalton Trans.*, 2781 (2003).
[2] A.J. Chmura, M.G. Davidson, M.D. Jones, M.D. Lunn, M.F. Mahon. *Dalton Trans.*, 887 (2006).
[3] C.J. Kepert. *Chem. Commun.*, 695 (2006).
[4] D. Maspoch, D.R. Molina, J. Veciana. *Chem. Soc. Rev.*, **36**, 770 (2007).
[5] K. Kuriki, Y. Koike, Y. Okamoto. *Chem. Rev.*, **102**, 2347 (2002).
[6] T. Terai, K. Kikuchi, S. Iwasawa, T. Kawabe, Y. Hirata, Y. Urano, T. Nagano. *J. Am. Chem. Soc.*, **128**, 6938 (2006).
[7] E.E.S. Teotonio, H.F. Brito, M.C.F.C. Felinto, L.C. Thompson, V.G. Young, O.L. Malta. *J. Mol. Struct.*, **751**, 85 (2005).
[8] R. Reyes, M. Cremona, E.E.S. Teotonio, H.F. Brito, O.L. Malta. *Chem. Phys. Lett.*, **396**, 54 (2004).
[9] J.G. Bünzli, C. Piguet. *Chem. Rev.*, **102**, 1897 (2002).
[10] R. Reyes, M. Cremona, E.E.S. Teotonio, H.F. Brito, O.L. Malta. *Thin Solid Films*, **469–470**, 59 (2004).
[11] W.A. Volkert, T.J. Hoffman. *Chem. Rev.*, **99**, 2269 (1999).
[12] G.J. Beyer, R. Offord, G. Künzi, Y. Aleksandrova, U. Ravn, S. Jahn, J. Barker, O. Tengblad, M. Lindroos. *Nucl. Med. Biol.*, **24**, 367 (1997).
[13] M. Neves, L. Gano, N. Pereira, M.C. Costa, M.R. Costa, M. Chandia, M. Rosado, R. Fausto. *Nucl. Med. Biol.*, **29**, 329 (2002).
[14] W. Fan, L.X. Chen, X.W. Liu, Q. Tang, S.F. Zhi, Z.Y. Zeng. *Chinese-German. J. Clin. Oncol.*, **6**, 396 (2007).
[15] V. Hušák, M. Mysliveček. *J. Radioanal. Nucl. Chem.*, **209**, 361 (1996).
[16] G.G. Skvortsov, M.V. Yakovenko, G.K. Fukin, E.V. Baranov, Yu.A. Kurskii, A.A. Trifonov. *Russ. Chem. Bull.*, **56**, 456 (2007).
[17] B. Yan, Q.Y. Xie. *Monatsh. Chem.*, **135**, 757 (2004).
[18] T. Toraishi, S. Nagasaki, S. Tanaka. *Theochem.*, **757**, 87 (2005).
[19] K. Miyoshi, J. Wang, T. Mizuta. *Bull. Chem. Soc. Japan*, **66**, 2547 (1993).
[20] K. Miyoshi, J. Wang, T. Mizuta. *Inorg. Chim. Acta*, **228**, 165 (1995).
[21] J. Wang, X.D. Zhang, Z.R. Liu, W.G. Jia. *J. Mol. Struct.*, **613**, 189 (2002).
[22] J. Wang, P. Hu, B. Liu, X. Chen, L.Q. Zhang, G.X. Han, R. Xu, X.D. Zhang. *Russ. J. Coord. Chem.*, **55**, 1 (2010).
[23] B. Liu, P. Hu, J. Wang, R. Xu, L.Q. Zhang, J. Gao, Y.F. Wang, X.D. Zhang. *Russ. J. Coord. Chem.*, **35**, 758 (2009).
[24] J. Wang, X. Zh. Liu, Zh.H. Zhang, X.D. Zhang, G.R. Gao, Y.M. Kong, Y. Li. *Russ. J. Coord. Chem.*, **32**, 590 (2006).
[25] X. Chen, D. Li, J. Wang, B. Liu, Y.M. Kong, D. Wang, X.D. Zhang. *J. Coord. Chem.*, **63**, 3897 (2010).
[26] J. Wang, D. Li, J.Q. Gao, B. Liu, B.X. Wang, D. Wang, T.T. Fan, X.D. Zhang. *J. Coord. Chem.*, **63**, 3792 (2010).
[27] L.J. Guggenberger, E.L. Muetterties. *J. Am. Chem. Soc.*, **98**, 7221 (1976).
[28] B. Liu, Y.F. Wang, J. Wang, J. Gao, R. Xu, Y.M. Kong, L.Q. Zhang, X.D. Zhang. *Russ. J. Coord. Chem.*, **50**, 917 (2009).
[29] J. Wang, Y. Wang, Z.H. Zhang, X.D. Zhang, X.Y. Liu, X. Zh. Liu, Zh.R. Liu, Y. Zhang, J. Tong, P. Zhang. *J. Coord. Chem.*, **59**, 295 (2006).